ChemPubSoc Europe

DOI: 10.1002/cmdc.201700602

CHEMMEDCHEM Full Papers

Nitrate Esters of Heteroaromatic Compounds as *Candida albicans* CYP51 Enzyme Inhibitors

Marija Smiljkovic,[a] Minos-Timotheos Matsoukas,[b, c] Eftichia Kritsi,[d] Urska Zelenko,[e] Simona Golic Grdadolnik,[e] Ricardo C. Calhelha,[f] Isabel C. F. R. Ferreira,[f] Snezana Sankovic-Babic,[g] Jasmina Glamoclija,[a] Theano Fotopoulou,[d] Maria Koufaki,[d] Panagiotis Zoumpoulakis,*[d] and Marina Sokovic*[a]

Four heteroaromatic compounds bearing nitrate esters were selected using a virtual-screening procedure as putative sterol 14α-demethylase (CYP51) *Candida albicans* inhibitors. Compounds were examined for their inhibition on *C. albicans* growth and biofilm formation as well as for their toxicity. NMR spectroscopy studies, in silico docking, and molecular dynamics simulations were used to investigate further the selectivity of these compounds to fungal CYP51. All compounds exhibited good antimicrobial properties, indicated with low minimal inhibitory concentrations and ability to inhibit formation of fungal biofilm. Moreover, all of the compounds had the ability to inhibit growth of *C. albicans* cells. *N*-(2-Nitrooxyethyl)-1*H*-indole-2-carboxamide was the only compound with selectivity on *C. albicans* CYP51 that did not exhibit cytotoxic effect on cells isolated from liver and should be further investigated for selective application in new leads for the treatment of candidiasis.

Introduction

Dimorphic yeast *Candida albicans* is among the most common fungal pathogens for humans causing different health problems from vaginal and oral infections to systemic and lethal candidiasis.[1] Fungal infection caused by *Candida* species has increased over the last years owing to immunosuppressed patients from HIV, organ transplantation, and cancer.[2] More than 17 different *Candida* species are known to be the cause of infections, and among them, *C. albicans*, *C. glabrata*, *C. parapsilosis*, *C. tropicalis*, and *C. crusei* are the main causes of more than 90% of invasive infections.[3]

Azole drugs, which usually constitute the first choice for antifungal therapy, act by inhibiting the sterol 14α-demethylase (CYP51) enzyme, which is involved in ergosterol biosynthesis. They bind to and inhibit the heme moiety of the enzyme, and this leads to depletion of ergosterol and the accumulation of toxic intermediates of ergosterol biosynthesis.[4] Azoles have been in clinical use since 1969,[5] and since then, numerous different compounds have been investigated and new compounds have been introduced. An increasing number of immunocompromised patients as well as increased resistance to azole drugs are the main reasons for further investigation of potential new antifungals.

During in silico screening of a small in-house chemolibrary, nitrate esters of heteroaromatic compounds were predicted to have the potential to inhibit the CYP51 *C. albicans* enzyme. Organic nitrate esters were previously shown to have antianginal activity, whereas their conjugates with nonsteroidal anti-inflammatory drugs (NSAIDs) are not ulcerogenic. However, the antimicrobial activity of this class of bioactive compounds has not been investigated. There is only one recent report by Kutty et al.[6] on nitrate esters possessing strong biofilm inhibition activity. To this end, in the present study, four nitrate esters were selected and evaluated in vitro for their binding and selectivity on candidal CYP51 and their consequent anticandidal activity. In addition, NMR spectroscopy studies, in silico docking, and molecular dynamics simulations were implemented to shed light on the binding mode of the proposed structures and to

[a] *M. Smiljkovic, Dr. J. Glamoclija, Dr. M. Sokovic*
Department of Plant Physiology, Institute for Biological Research "Siniša Stanković", University of Belgrade, Bulevar Despota Stefana 142, 11000 Belgrade (Serbia)
E-mail: mris@ibiss.bg.ac.rs

[b] *Dr. M.-T. Matsoukas*
Cloudpharm P.C., Monumental Plaza, Building C, Kifissias Avenue 44, Marousi, 15125 Athens (Greece)

[c] *Dr. M.-T. Matsoukas*
Department of Pharmacy, University of Patras, 26500 Rio, Patras (Greece)

[d] *Dr. E. Kritsi, Dr. T. Fotopoulou, Dr. M. Koufaki, Dr. P. Zoumpoulakis*
National Hellenic Research Foundation, Institute of Biology, Medicinal Chemistry and Biotechnology, Vas. Constantinou Ave. 48, 11635 Athens (Greece)
E-mail: pzoump@eie.gr

[e] *Dr. U. Zelenko, Dr. S. G. Grdadolnik*
Department of Biomolecular Structure, National Institute of Chemistry, Hajdrihova ulica 19, 1000 Ljubljana (Slovenia)

[f] *Dr. R. C. Calhelha, Dr. I. C. F. R. Ferreira*
Mountain Research Centre (CIMO, ESA), Polytechnic Institute of Bragança, Campus de Santa Aplónia, 5300253 Bragança (Portugal)

[g] *Dr. S. Sankovic-Babic*
ENT Clinic, Clinical Hospital Centre Zvezdara, Presevska 31, Belgrade (Serbia)

Supporting Information and the ORCID identification number(s) for the author(s) of this article can be found under: https://doi.org/10.1002/cmdc.201700602.

provide information regarding the observed differences in activity.

Results and Discussion

Selection of compounds

Virtual screening was performed by using a high-throughput docking algorithm (Glide HTVS) on the homology model of the *C. albicans* CYP51 enzyme. The four compounds were selected on the basis of their ability to interact with heme iron, their ability to interact with crucial amino acids of the active site, and their scoring values. The docked poses of each of the selected compounds are presented in Figure S1 (Supporting Information), and the corresponding docking scores are shown in Table S1.

Anticandidal activity of selected compounds

The anticandidal activity of selected compounds is presented in Table 1. All of the *C. albicans* clinical isolates were susceptible to the tested compounds with similar susceptibility. Good antifungal activity of the compounds (average minimal inhibitory concentration of 0.0028 mg mL^{-1} and minimal fungicidal concentration of 0.0056 mg mL^{-1}) was recorded. Compound MK94 had the strongest inhibitory activity toward *C. albicans* followed by MK56. The commercial drug ketoconazole was used as a positive control, and it showed lower inhibitory and fungicidal concentrations than the tested compounds.

Antibiofilm activity of selected compounds

The impact on biofilm formation was anti-quorum sensing trait detected for all of the tested compounds, and MK56 showed the strongest effect with 80% inhibition at the minimum inhibitory concentration (MIC) and 87% at $^1/_2$ MIC. Ketoconazole together with MK55 also had strong activity on biofilm formation, and at the MIC they showed 80 and 73% inhibition, respectively, and at $^1/_2$ MIC showed 73 and 61% inhibition, respectively (Table 2).

Table 2. Percent inhibition of biofilm formation after treatment with minimal inhibitory and sub-inhibitory concentrations of test compounds.

Compound	Inhibition [%]			
	MIC	$^1/_2$ MIC	$^1/_4$ MIC	$^1/_8$ MIC
MK55	73	61	27	–
MK56	80	87	74	54
MK94	45	15	–	–
MK129	56	48	14	11
ketoconazole	80	73	71	52

Binding affinities on CYP51 enzyme

Different concentrations of compounds were incubated with the CYP51 enzyme isolated from *C. albicans* and also the human and bovine CYP51 enzymes. The recorded binding spectra show that MK55 binds to the CYP51 enzyme isolated from *C. albicans* with a dissociation constant (K_D) of 4.19 μM (Figure 1 A), whereas the other tested compounds, MK56, MK94, and MK129, do not exhibit any binding affinity toward the CYP51 enzyme, which is indicative of a different mode of action. Given that MK55 binds to the candidal enzyme, it was tested for selectivity on human and bovine CYP51 enzymes, and it showed good selectivity only to candidal CYP51 (Figure 1 B). The commercial antifungal drug ketoconazole was also tested, and it showed dissociation constants <0.05 μM for CYP51 isolated from *C. albicans* and <0.05 μM for human CYP51.

NMR spectroscopy studies

The binding of MK55 to CYP51 isolated from *C. albicans* was further investigated at the atomic level by the application of 1 D saturation-transfer difference (STD) and 2 D transferred NOESY NMR experiments in D_2O buffer. STD effects were observed for all of the carbon-bound protons, and this indicates

Table 1. Antifungal activity of tested compounds.[a]

Compd	*C. albicans* 475/15		*C. albicans* 527/14		*C. albicans* 10/15		*C. albicans* 13/15	
	MIC	MFC	MIC	MFC	MIC	MFC	MIC	MFC
MK55	0.056 ± 0.001	0.112 ± 0.002	0.028 ± 0.001	0.056 ± 0.002	0.056 ± 0.001	0.112 ± 0.01	0.028 ± 0.001	0.056 ± 0.001
	224.692 ± 4.01	449.384 ± 8.02	112.346 ± 4.01	224.692 ± 8.02	224.692 ± 4.01	449.384 ± 40.12	112.346 ± 4.01	224.692 ± 4.01
MK56	0.028 ± 0.001	0.056 ± 0.001	0.028 ± 0.001	0.056 ± 0.001	0.056 ± 0.001	0.112 ± 0.01	0.028 ± 0.001	0.056 ± 0.002
	107.181 ± 3.83	214.362 ± 3.83	107.181 ± 3.83	214.362 ± 3.83	214.362 ± 3.83	428.725 ± 38.28	107.181 ± 3.83	214.362 ± 7.66
MK129	0.056 ± 0.001	0.122 ± 0.002	0.028 ± 0.001	0.056 ± 0.001	0.056 ± 0.002	0.112 ± 0.01	0.028 ± 0.001	0.056 ± 0.002
	179.349 ± 3.2	390.725 ± 6.41	89.675 ± 3.2	179.349 ± 3.2	179.349 ± 6.41	358.698 ± 32.03	89.675 ± 32.03	179.349 ± 6.41
MK94	0.028 ± 0.002	0.056 ± 0.001	0.028 ± 0.002	0.056 ± 0.002	0.028 ± 0.001	0.056 ± 0.002	0.028 ± 0.002	0.056 ± 0.002
	80.149 ± 5.72	160.298 ± 2.86	80.149 ± 5.72	160.298 ± 5.72	80.149 ± 2.86	160.298 ± 5.72	80.149 ± 5.72	160.298 ± 5.72
keto	0.0031 ± 0.0001	0.0062 ± 0.0001	0.00312 ± 0.0001	0.00625 ± 0.0001	0.0031 ± 0.0001	0.05 ± 0.0001	0.0016 ± 0.0002	0.05 ± 0.0002
	5.833 ± 0.19	11.667 ± 0.19	5.871 ± 0.19	11.761 ± 0.19	5.833 ± 0.19	94.086 ± 0.19	3.011 ± 0.38	94.086 ± 0.38

[a] MIC: minimum inhibitory concentration; MFC: minimum fungicidal concentration; results are expressed in mg mL^{-1} (top row) and in μM (bottom row) for each compound and strain. Values are the mean ± SD of $n=3$ experiments. In all cases, MIC and MFC values for test compounds were found to be significantly different ($p<0.05$) from those of the positive control, ketoconazole (keto).

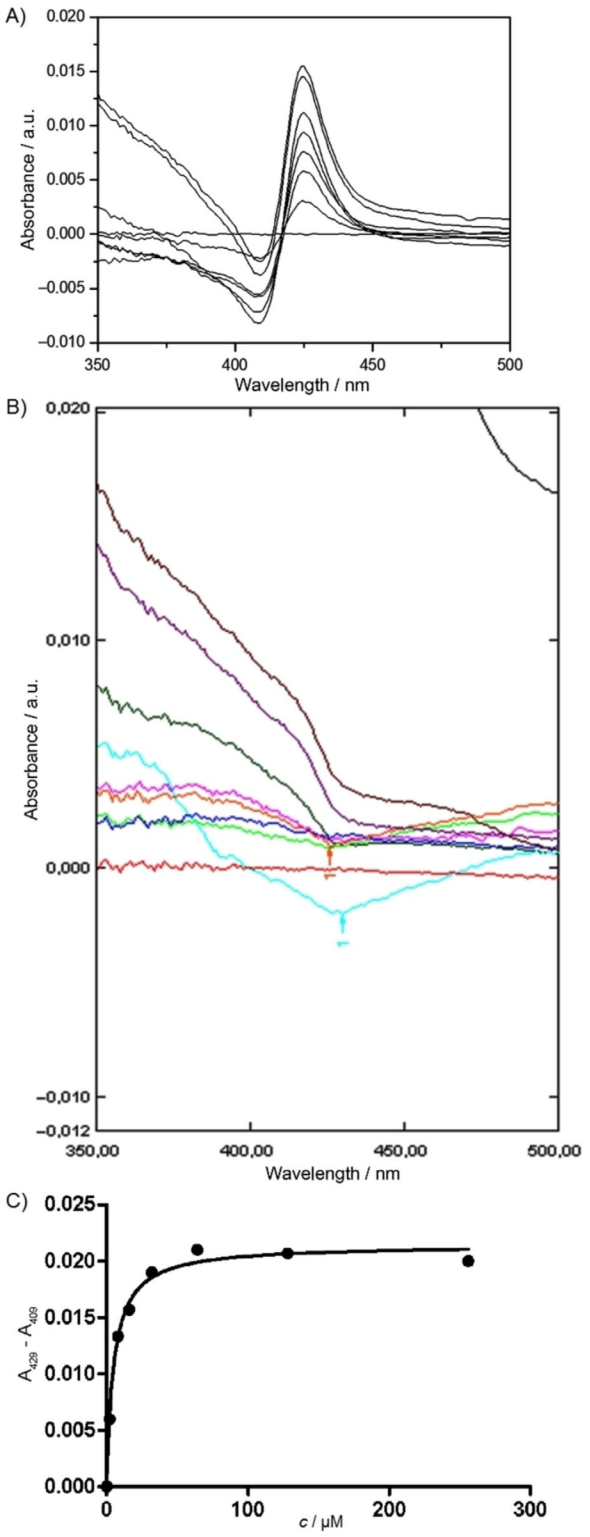

Figure 1. Binding spectra in the $\lambda = 350–500$ nm range recorded after titrating A) *C. albicans* and B) human enzyme with increasing concentrations of MK55; C) saturation curve of MK55.

that MK55 is buried inside the enzyme and provides contact to all proton-rich moieties with the protein. A sign change in the ligand NOE cross-peaks is observed upon the addition of the enzyme in the NOESY spectrum of MK55, which is typically observed for ligand–enzyme binding. In the NOESY spectrum of MK55 recorded in the absence of the enzyme, only trivial positive NOE cross-peaks are observed. In the transferred NOESY spectrum of MK55 in the presence of the enzyme, besides the strong negative trivial NOE cross-peaks, weak negative NOE cross-peaks between the H3 proton of the indole ring and the methylene protons of the ethyl spacer are observed. This is the only difference between the NOE patterns of the free and bound ligand states and is indicative of different relative orientations of the nitrooxyethyl moiety with respect to the indole ring in the two ligand states. In the ligand-bound state, the methylene protons of the nitrooxyethyl moiety are in close spatial proximity (< 5 Å) to the H3 proton of the indole ring (Figure 2).

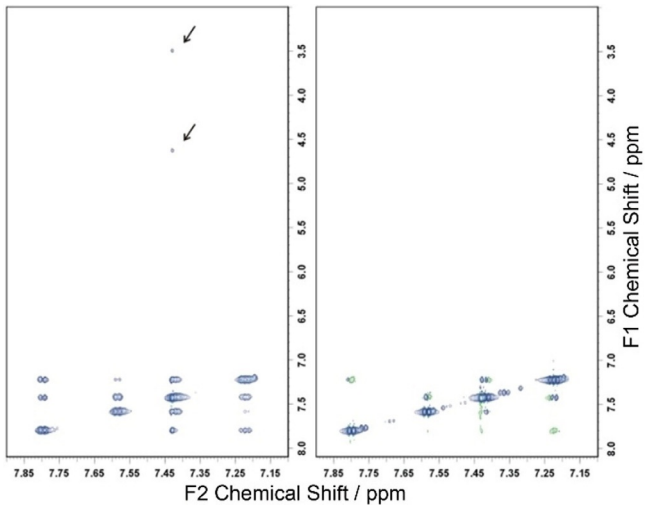

Figure 2. Expanded regions of the transferred NOESY spectrum (left) of MK55 in the presence of CYP51 isolated from *C. albicans* and the NOESY spectrum (right) of MK55 recorded in the absence of the enzyme. The observed weak negative NOE cross-peaks between the H3 proton ($\delta = 7.43$ ppm) of the indole ring and the methylene protons ($\delta = 4.63$ and 3.49 ppm) of the ethyl spacer are indicated with arrows.

Molecular docking studies

A structural model of *C. albicans* CYP51 was prepared on the basis of the crystal structure of *Saccharomyces cerevisiae* CYP51 (Figure 3) to perform docking of MK55 and to evaluate its binding affinity with respect to the experimental one. MK55 was the only compound that was experimentally found to bind selectively to *C. albicans* CYP51. For comparison reasons, MK56 was also docked, as it shares common structural features with MK55 but fails to bind *C. albicans* CYP51 as presented above. The commercial antifungals voriconazole and ketoconazole, with already known affinity to CYP51, were also tested in silico to compare and validate the MK55 and MK56 docking results. Voriconazole showed a docking pose identical to the previously determined voriconazole crystal structures to other CYP51 cytochromes (PDB IDs: 5HS1, 4ZE0, and 4UYM). Similarly, the highest scored pose of ketoconazole was in agreement with previous ketoconazole–CYP51 crystal structures (PDB IDs: 3LD6 and 2JJP). MK55 and MK56 showed similar docking poses

Figure 3. Sequence alignment between *Saccharomyces cerevisiae* CYP51 and *C. albicans* CYP51. Blue color intensity corresponds to amino-acid sequence similarity.

in the heme prosthetic group region surrounded by Y118, L121, T122, F126, Y132, L139, F228, G307, L376, and M508.

Molecular dynamics simulations

To evaluate further the binding mode and stability, complexes of voriconazole, ketoconazole, MK55, and MK56 with CYP51 were subjected to unconstrained molecular dynamics simulations for 200 ns each. For three of the compounds, that is, voriconazole, ketoconazole, and MK55, the docking pose was stable through the molecular dynamics simulations, depicting a rather consistent topology. The distances of the imidazole nitrogen atom and nitro group oxygen atoms (center of mass) to the iron atom were monitored to evaluate the consistency of the interaction with the Fe atom (Figure 4A). The results indicate that the indole nitrogen atom of ketoconazole has a constant interaction with the heme iron at approximately 2 Å, whereas the indole nitrogen atom of voriconazole does not, at least after approximately the first 50 ns; however, the indole nitrogen atom is in constant proximity of approximately 3 Å. For the case of MK55, the nitro group remains stable for most of the simulation time and has a distance of 2–3 Å to the iron atom, but this is not observed for MK56, for which the nitro group does not maintain its interaction with Fe.

Ketoconazole has a higher binding affinity for CYP51 than for MK55. The docking and subsequent molecular dynamics (MD) simulations showed a very stable topology for this compound, which forms several hydrophobic interactions with the cytochrome protein. Specifically, the imidazole group interacts with L376; the dichlorophenyl group interacts with I131, F126, and Y132; the dioxolane ring interacts with Y118 and F228; the phenyl group interacts with F235, F380, and M508; and the piperazine group interacts with the Y64, H377, and F380 hydrophobic side chains (Figure 4B). Likewise, MK55 has a stable interaction with the heme iron and forms several interactions, especially with F126, Y118, M508, and V509 (Figure 4C). Important interactions include the indole ring, which is stabilized by the aromatic side-chain ring of F228, and the aliphatic chain of L121. The methylene protons of the nitrooxyethyl moiety were also monitored for their proximity to the H3 proton of MK55, as observed by the NOE cross-peaks (Figure 2), and were found to be consistent with the NMR spectroscopy data (Figure 4D). The set of interactions that govern this position of MK55 with the *C. albicans* CYP51 pocket is highlighted in Figure 4E. The phenyl ring from the indole group, interacting with L376, L121, T311, M508, and V509, seems to play the most significant role in the binding of MK55. If superimposed, MK55 and ketoconazole have similar topologies in the interaction site and relative to the heme cofactor (Figure 4F)

Cytotoxicity of *N*-(2-nitrooxyethyl)-1*H*-indol-2-carboxamide (MK55)

MK55 was tested in a cytotoxicity assay on PLP2 cells, as it was the only one with proposed mode of action on *C. albicans*. MK55, with median growth inhibition (GI_{50}) values $>400\ \mu g\,mL^{-1}$, did not present cytotoxic activity relative to ellipticine, which was used as a positive control ($GI_{50}=3.22\ \mu g\,mL^{-1}$).

Conclusions

Four nitrate esters were selected from an in-house chemical library and were tested for their activity toward four different strains of *C. albicans*. All compounds exhibited moderate to good antifungal activities, although the activities were still lower than that of the commercial antifungal drug ketoconazole. The compounds also presented identical susceptibility. Two of the tested nitrate esters, namely, MK56 and to a lesser extent MK55, exhibited good inhibition effects on biofilm formation and can be considered as novel anti-quorum sensing agents.

Although all four compounds exhibited moderate to good anti-candidal activities in vitro, their mechanisms of action are different. Among the four tested compounds, only MK55 bound to CaCYP51 through interaction with heme Fe, which indicated that its mode of action was related to inhibition of ergosterol biosynthesis. The dissociation constant (K_D) of MK55 for the candidal enzyme was higher than that of ketoconazole, which indicated lower binding affinity of MK55. Furthermore, NMR spectroscopy studies, in silico docking, and molecular dynamics simulations revealed a putative binding pose for MK55, proposing a metal coordination complex that was not present for the case of the other nitrate esters.

Most importantly, this study revealed that MK55 selectively binds *C. albicans* with no activity to human CYP51, whereas ketoconazole is not selective toward the fungal enzyme and has a low K_D for human CYP51. This is in accordance with previous investigations, for which it was concluded that ketoconazole had a hepatotoxic side effect,[7] probably as a consequence of nonspecific binding. Moreover, as one of the most common side effects of azole drugs is liver damage,[8] MK55 toxicity was tested on the PLP2 cell line from pig's liver, and it presented no cytotoxic effects. From the above findings, it is concluded that MK55 [(*N*-(2-nitrooxyethyl)-1*H*-indol-2-carboxamide] could

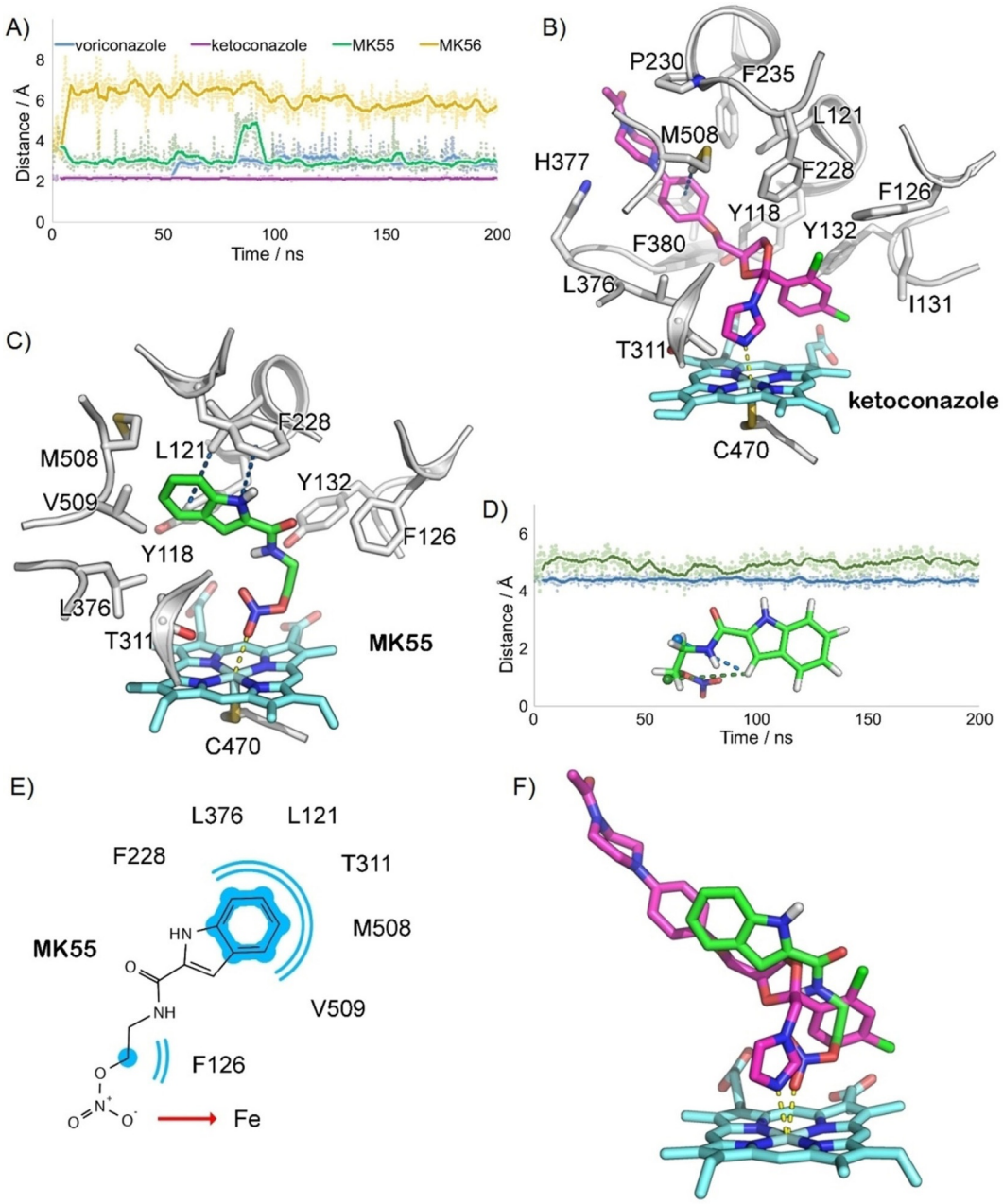

Figure 4. A) Distances monitored during the molecular dynamics simulations between the imidazole nitrogen atom (vericonazole and ketoconazole) or nitro group oxygen atoms center of mass (MK55 and MK56) to the heme iron. B) Representative binding pose of ketoconazole (in magenta stick representation) to CYP51 (gray). C) Representative binding pose of MK55 (in green stick representation) to CYP51 (gray). Electrostatic interactions are shown in yellow and certain hydrophobic interactions are shown in blue. D) Distances during the molecular dynamics simulations between H3 of MK55 and the methylene hydrogen atoms center of mass of the ethyl spacer. E) MK55 pharmacophoric groups and their proximal interacting residues in a 2D representation. Hydrophobic interactions are highlighted in blue. F) Superimposition of ketoconazole (magenta) and MK55 (green) with respect to the heme cofactor.

be further investigated as a potential antifungal lead for future development of novel antifungal compounds.

Experimental Section

Synthesis

Nitrogen heterocyclic compounds: The synthesis of the nitrate esters of the heteroaromatic compounds (MK55, MK56, MK94, and MK129) was previously described.[9,10] *N*-(2-Nitrooxyethyl)-1*H*-indole-2-carboxamide (MK55), *N*-(2-nitrooxyethyl)-quinoline-2-carboxamide (MK56), *N*-(2-nitrooxyethyl)-6-(piperidin-1-yl)-9*H*-purine acetamide (MK94), and 5′-*O*-nitroadenosine (MK129) were the subjects of investigation (Scheme 1).

Biological methods

Microbial culture conditions: Four strains of *C. albicans* were used in this study. Isolates were isolated from oral cavities of patients at ENT Clinic, Clinical Hospital Centre Zvezdara, Belgrade, Serbia, by

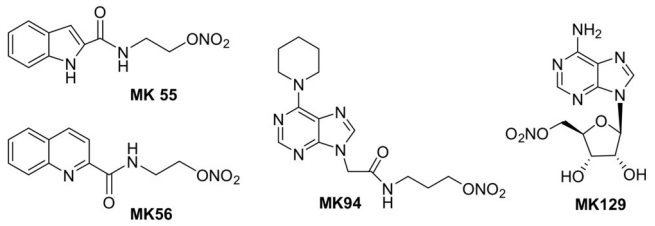

Scheme 1. Compounds tested in this study.

rubbing a sterile cotton swab upon obtaining informed written consent. Strains were determined on CHROMagar plates (Biomerieux, France). *C. albicans* strains were maintained on Sabourand Dextrose Agar (Merck, Germany) at 4 °C and were subcultured once a month.

Anticandidal activity of selected compounds: Minimum inhibitory concentrations (MICs) and minimum fungicidal concentrations (MFCs) were established by the use of the microdilution standardized technique[11] with modification. In brief, with the use of sterile saline, fresh overnight yeast cultures were adjusted to a concentration 1.0×105 CFU well^{-1}. The microplates were incubated at 37 °C for 24 h, after which the MIC and MFC were determined.

The MIC values were considered as the lowest concentrations without microscopically observed growth. Following the serial subcultivations of 10 μL into microtiter plates containing 100 μL of broth per well, as well as subsequent incubation at 37 °C for 24 h, the lowest concentrations with no visible growth were defined as the MFC values, indicating 99.5% killing of the original inoculum.[12] Ketoconazole was used as a positive control (Sigma–Aldrich, Germany).

Antibiofilm activity of selected compounds: Impact of azole compounds on biofilm formation was determined as described[13] with some modifications. *C. albicans* cells were incubated for 24 h in 96-well microtiter plates with an adhesive bottom (Sarstedt, Germany) at 37 °C with MIC and subMIC concentrations of the compounds. After 24 h, each well was washed twice with sterile PBS (phosphate-buffered saline, pH 7.4). Fixation of adhered cells was done with methanol, after which the plate was air dried and stained with 0.1% crystal violet (Bio-Merieux, France) for 30 min. Wells were washed with water to remove any unbound stain and were air dried, and then 96% ethanol (100 μL) was added (Zorka, Serbia) to suspend all the bound stain. Absorbance was read at $\lambda=$ 620 nm with a Multiskan FC Microplate Photometer (Thermo Scientific). Percentage of inhibition of biofilm formation was calculated by using Equation (1):

$$\frac{(A_{620\ \text{control}}-A_{620\ \text{sample}})}{A_{620\ \text{control}}}\times 100 \qquad (1)$$

Analytical methods

UV/Vis spectra and ligand binding: Sterol 14α-demethylase (CYP51) from *C. albicans*, human, and bovine was previously isolated at the Laboratory of Biomolecular Structure at the National Institute of Chemistry, Ljubljana, Slovenia.[14] Spectra were taken at room temperature by using a double-beam Shimadzu UV-1800 spectrophotometer. For ligand binding, 1 μM of human, bovine, or *C. albicans* CYP51 in 50 mM phosphate buffer (pH 7.4), 100 mM NaCl, and 10% glycerol were progressively titrated with investigated ligands at concentrations of 0, 2, 8, 16, 32, 64, 128, 256, and 300 μM. After each incremental addition of the ligand, an equivalent volume of solvent was added to the reference cuvette. Spectra were recorded from $\lambda=350$ to 500 nm, and ligand-induced spectral changes were monitored as difference type II spectral responses. Each binding assay was repeated three times. Plots of absorbance changes against ligand concentration were constructed, and the apparent dissociation constants (K_D) were determined by nonlinear regression in GraphPad Prism version 5.04 for Windows (GraphPad Software, San Diego California USA) by using Equation (2):

$$\Delta A=\Delta A_{max}\times\frac{[L]}{K_D+[L]} \qquad (2)$$

in which ΔA is the peak-to-trough absorbance change in the difference spectra, ΔA_{max} is the maximum absorbance change, $[L]$ is the concentration of the ligand used for the titration, and K_D is the dissociation constant for the ligand–enzyme complex.

NMR spectroscopy: High-resolution NMR spectra were recorded by using a Varian DirectDrive 800 MHz spectrometer at 25 °C. All data were collected by using pulse sequences and phase-cycling routines provided in Varian libraries of pulse programs. A cryogenic triple-resonance NMR probe was used. NMR samples for the STD and transferred NOESY experiments were prepared in a buffer containing 20 mM [D_{11}]Tris, 10% [D_8]glycerol, and 100 mM NaCl in D_2O, pD 7.2. 0.1 mM 4,4-dimethyl-4-silapentane-1-sulfonic acid (DSS) was used as an internal standard. All spectra were recorded at a protein/ligand ratio of 1:100, the protein concentration was 8 μM, and the ligand concentration was 0.8 mM.

Transferred NOESY[15,16] spectra were acquired with an 8802.8 Hz spectral width, 4096 data points in t_2, 16 scans, 180–256 complex points in t_1, a relaxation delay of 1.5 s, and mixing times of 200 and 300 ms. The residual water signal was suppressed by using excitation sculpting,[17,18] and adiabatic pulses[19] were applied for the suppression of zero quantum artefacts during the mixing time. A $T_1\rho$ filter of 30 ms was used to eliminate the background protein resonance. The spectrum was processed and analyzed with the FELIX 2007 software package from Felix NMR, Inc. The spectrum was zero-filled twice and apodized with a squared sine bell function shifted by $\pi/2$ in both dimensions.

The STD experiment[20] was performed with an 8802.8 Hz spectral width, 16384 data points, a saturation time of 300 ms, a relaxation delay of 6.3 s, and 6000 scans. Saturation time and relaxation delay were selected according to the shortest and longest ^{1}H T_1 relaxation times of the ligand to attain the experimental conditions for quantitative STD measurements.[21] Selective saturation was achieved by a train of 50 ms long Gauss-shaped pulses separated by 1 ms delay. Water was suppressed by excitation sculpting. The on-resonance selective saturation of CYP51 was applied at $\delta=$ −0.38 ppm. The off-resonance irradiation was applied at $\delta=$ 30 ppm for the reference spectrum. Subtraction of the on- and off-resonance spectra was performed internally by phase cycling. The spectrum was zero-filled twice and apodized by an exponential line-broadening function of 1 Hz.

Modeling studies

Preparation of CYP51, virtual screening, and molecular docking: Production of the *C. albicans* CYP51 protein structural model (Uniprot code P10613) was made by homology modeling with MODELLER 9.17[22] by using the crystal structure of *Saccharomyces cerevi-*

siae CYP51 complexed with fluquinconazole (PDB ID: 5EAF) as a template. The two sequences share 65% identity. Gaps and insertions between residues in the alignment were only introduced in loop regions. Twenty models were produced, and their overall stereochemical quality was evaluated by means of visual inspection and the discrete optimized energy (DOPE)[23] to conclude to the final model.

For the virtual screening process, all compounds from the in-house library were primarily sketched and prepared at pH 7.5±0.5 with LigPrep of Maestro (LigPrep, Schrödinger, LLC, New York, NY, 2017). For the CYP51 modeled receptor, the Fe^{II} ion formal charge was set to +2. Subsequently, the examined library was screened by using Glide High Throughput Virtual Screening (Glide HTVS)—Precision mode, Maestro, version 11.2.013 (Glide, Schrödinger, LLC, New York, NY, 2017).[24–26] For the explanatory docking, selected compounds were flexibly docked into the binding sites of the receptor by using AutoDock Vina.[27] The AutoDockTools program was used to prepare the corresponding PDBQT–protein file. The receptor was held rigid during the docking process, whereas the ligand was allowed to be flexible. Docking simulations in both cases were performed by using a grid box with dimensions of 25 25 25 Å, a search space of 20 binding modes, and the search parameter was set to 5. The best docking pose for each compound was selected on the basis of the lowest energy docked conformation.

Molecular dynamics simulations: All MD simulations were performed by using the GROMACS software v 5.1.[28] Following the structural model, minimization of the receptor topology was performed to remove steric clashes between the residues. The minimized topology was then inserted in a pre-equilibrated box containing water and a 0.15 M concentration of Na and Cl ions. The latest AMBER99SB-ILDN[29] force field was used for all of the dynamics simulations along with the TIP3P water model. Force-field parameters for the ligands were generated by using the general Amber force field (GAFF) and HF/6-31G*-derived RESP atomic charges.[30] AMBER-compatible heme parameters were derived from elsewhere.[31] Each system consisted of the protein, the ligand, ≈15000 water molecules, and ≈160 ions in a 10×10×10 nm simulation box. The model systems were energy minimized and subsequently subjected to a 10 ns MD equilibration, with positional restraints on protein coordinates. These restraints were released, and 200 ns MD trajectories were produced at a constant temperature of 300 K by using separate v-rescale thermostats for the protein, the peptide, and solvent molecules. A time step of 2 fs was used, and all bonds were constrained by using the LINCS algorithm. Lennard–Jones interactions were computed by using a cutoff of 10 Å, and the electrostatic interactions were treated by using PME with the same real-space cutoff.

Cytotoxicity of compounds in a porcine liver primary cell culture: A cell culture was prepared from a freshly harvested porcine liver obtained from a local slaughter house, and it was designed as PLP2. Briefly, the liver tissues were rinsed in Hank's balanced salt solution containing 100 U mL^{-1} penicillin and 100 μg mL^{-1} streptomycin and were divided into 1×1 mm^3 explants. Some of these explants were placed in 25 cm^2 tissue flasks in Dulbecco's modified Eagle's medium (DMEM) supplemented with 10% fetal bovine serum (FBS), 2 mM nonessential amino acids, 100 U mL^{-1} penicillin, and 100 mg mL^{-1} streptomycin and were incubated at 37 °C with a humidified atmosphere containing 5% CO_2. The medium was changed every 2 d. Cultivation of the cells was continued with direct monitoring every 2–3 days by using a phase-contrast microscope. Before confluence was reached, cells were subcultured and plated in 96-well plates at a density of 1.0×10^4 cells per well and were cultivated in DMEM with 10% FBS, 100 U mL^{-1} penicillin, and 100 μg mL^{-1} streptomycin. Sulforhodamine B assay was performed according to a procedure previously described.[32] The results were expressed in GI_{50} values (compound concentration that inhibited 50% of the net cell growth). Ellipticine was used as a positive control.

Acknowledgements

This work was supported financially by the Serbian Ministry of Education, Science, and Technological Development (Grant number 173032). Binding studies to CaCYP51 were supported by the Slovenian Research Agency (Grants P1-0010 and J1-8145) and by a program of scientific and technological cooperation between the Republic of Serbia and the Republic of Slovenia "A combined methodology towards the development of novel, selective inhibitors of Candida CYP51".

Conflict of interest

The authors declare no conflict of interest.

Keywords: antimicrobial activity · biofilms · inhibitors · nitrate esters · virtual screening

[1] F. L. Mayer, D. Wilson, B. Hube, *Virulence* **2013**, *4*, 119–128.
[2] P. Vandeputte, S. Ferrari, A. T. Coste, *Int. J. Microbiol.* **2012**, 713687.
[3] J. C. Sardi, L. Scorzoni, T. Bernardi, A. M. Fusco-Almeida, M. J. M. Giannini, *J. Med. Microbiol.* **2013**, *62*, 10–24.
[4] M. Bondaryk, W. Kurzatkowski, M. Staniszewska, *Postepy Dermatol. Alergol.* **2013**, *5*, 293–301.
[5] R. A. Fromtling, *Clin. Microbiol. Rev.* **1988**, *1*, 187–217.
[6] S. K. Kutty, N. Barraud, A. Pham, G. Iskander, S. A. Rice, D. S. Black, N. Kumar, *J. Med. Chem.* **2013**, *56*, 9517–9529.
[7] J. Y. Yan, X. L. Nie, Q. M. Tao, S. Y. Zhan, Y. D. Zhang, *Biomed. Environ. Sci.* **2013**, *26*, 605–610.
[8] B. Elewski, A. Tavakkol, *Ther. Clin. Risk Manage.* **2005**, *1*, 299–306.
[9] T. Fotopoulou, E. K. Iliodromitis, M. Koufaki, A. Tsotinis, A. Zoga, V. Gizas, A. Pyriochou, A. Papapetropoulos, I. Andreadou, D. T. Kremastinos, *Bioorg. Med. Chem.* **2008**, *16*, 4523–4531.
[10] M. Koufaki, T. Fotopoulou, E. K. Iliodromitis, S. I. Bibli, A. Zoga, D. T. Kremastinos, I. Andreadou, *Bioorg. Med. Chem.* **2012**, *20*, 5948–5956.
[11] EUCAST, European Committee on Antibiotic Susceptibility. Discussion document E. Dis. 7.1. Taufkirchen: European Society of Clinical Microbiology and Infectious Diseases, **2002**.
[12] T. Tsukatani, H. Suenaga, M. Shiga, K. Noguchi, M. Ishiyama, T. Ezoe, K. Matsumoto, *J. Microbiol. Methods* **2012**, *90*, 160–166.
[13] C. G. Pierce, P. Uppuluri, A. R. Tristan, F. L. Wormley, Jr., E. Mowat, G. Ramage, J. L. Lopez-Ribot, *Nat. Protoc.* **2008**, *3*, 1494–1500.
[14] U. Zelenko, M. Hodoscek, D. Rozman, S. G. Grdadolnik, *J. Chem. Inf. Model.* **2014**, *54*, 3384–3395.
[15] G. M. Clore, A. M. Gronenborn, *J. Magn. Reson. (1969–1992)* **1982**, *48*, 402–417.
[16] G. M. Clore, A. M. Gronenborn, *J. Magn. Reson. (1969–1992)* **1983**, *53*, 423–442.
[17] C. Dalvit, *J. Biomol. NMR* **1998**, *11*, 437–444.
[18] T. L. Hwang, A. J. Shaka, *J. Magn. Reson. Ser. A* **1995**, *112*, 275–279.
[19] M. J. Thrippleton, J. Keeler, *Angew. Chem. Int. Ed.* **2003**, *42*, 3938–3941; *Angew. Chem.* **2003**, *115*, 4068–4071.
[20] M. Mayer, B. Meyer, *J. Am. Chem. Soc.* **2001**, *123*, 6108–6117.
[21] J. Yan, A. D. Kline, H. Mo, M. J. Shapiro, E. R. Zartler, *J. Magn. Reson.* **2003**, *163*, 270–276.

[22] B. Webb, A. Sali in *Current Protocols in Bioinformatics*, Wiley, New York, **2014**, *47*, 5.6.1 – 5.6.32.
[23] M. Y. Shen, A. Sali, *Protein Sci.* **2006**, *15*, 2507 – 2524.
[24] R. A. Friesner, R. B. Murphy, M. P. Repasky, L. L. Frye, J. R. Greenwood, T. A. Halgren, P. C. Sanschagrin, D. T. Mainz, *J. Med. Chem.* **2006**, *49*, 6177 – 6196.
[25] T. A. Halgren, R. B. Murphy, R. A. Friesner, H. S. Beard, L. L. Frye, W. T. Pollard, J. L. Banks, *J. Med. Chem.* **2004**, *47*, 1750 – 1759.
[26] R. A. Friesner, J. L. Banks, R. B. Murphy, T. A. Halgren, J. J. Klicic, D. T. Mainz, M. P. Repasky, E. H. Knoll, D. E. Shaw, M. Shelley, J. K. Perry, P. Francis, P. S. Shenkin, *J. Med. Chem.* **2004**, *47*, 1739 – 1749.
[27] O. Trott, A. J. Olson, *J. Comput. Chem.* **2010**, *31*, 455 – 461.
[28] M. J. Abraham, T. Murtola, R. Schulz, S. Páll, J. C. Smith, B. Hess, E. Lindahl, *SoftwareX*, **2015**, *1*, 19 – 25.
[29] K. Lindorff-Larsen, S. Piana, K. Palmo, P. Maragakis, J. L. Klepeis, R. O. Dror, D. E. Shaw, *Proteins Struct. Funct. Bioinf.* **2010**, *78*, 1950 – 1958.
[30] C. I. Bayly, P. Cieplak, W. Cornell, P. A. Kollman, *J. Phys. Chem.* **1993**, *97*, 10269 – 10280.
[31] K. Shahrokh, A. Orendt, G. S. Yost, T. E. Cheatham III, *J. Comput. Chem.* **2012**, *33*, 119 – 133.
[32] R. Guimaraes, L. Barros, M. Duenas, R. C. Calhelha, A. M. Carvalho, C. Santos-Buelga, M. J. Queiroz, I. C. F. R. Ferreira, *Food Chem.* **2013**, *136*, 718 – 725.

Manuscript received: September 27, 2017
Revised manuscript received: November 8, 2017
Accepted manuscript online: December 13, 2017
Version of record online: January 26, 2018